IEEE Photonics Journal
An IEEE Photonics Society Publication

Open Access

Chip-Asynchronous Binary Optical CDMA: An Optimum Signaling Scheme for Random Delays

Volume 5, Number 2, April 2013

Salman A. Khan
Jan Bajcsy

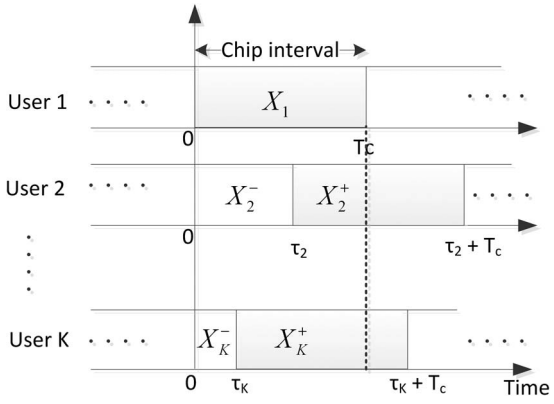

DOI: 10.1109/JPHOT.2013.2255033
1943-0655/$31.00 ©2013 IEEE

IEEE photonics SOCIETY

IEEE

Chip-Asynchronous Binary Optical CDMA: An Optimum Signaling Scheme for Random Delays

Salman A. Khan and Jan Bajcsy

Department of Electrical and Computer Engineering, McGill University, Montreal, QC H3A 2A7, Canada

DOI: 10.1109/JPHOT.2013.2255033
1943-0655/$31.00 ©2013 IEEE

Manuscript received March 18, 2013; accepted March 19, 2013. Date of publication March 27, 2013; date of current version April 9, 2013. This work was supported in part by the Natural Sciences and Engineering Research Council (Canada) and in part by the Fonds de Recherché Nature et Technologies (FQRNT) Doctoral Scholarship. Corresponding author: S. A. Khan (e-mail: salman.khan2@mail.mcgill.ca).

Abstract: Most optical code division multiple access (OCDMA) research literature has focused on *chip-synchronous* OCDMA. However, practical OCDMA networks are inherently *chip-asynchronous* since users transmit their signals from different locations without any coordination. This paper focuses on binary *chip-asynchronous* OCDMA with time spreading, and the main result is that appropriate nonuniform signaling can achieve a data throughput of 2.5 bits per OCDMA chip. This result shows that the presence of *chip asynchronism* leads to approximately a threefold capacity gain over *chip-synchronous* OCDMA capacity. Additional results are presented to illustrate that the near capacity multiuser interference has a low variance and a non-Gaussian distribution. Finally, the robustness of the achieved capacity gains is verified in the presence of additive channel noise.

Index Terms: Optical code division multiple access (OCDMA), nonuniform signaling, chip asynchronism, channel capacity.

1. Introduction

Flexibility of having an asynchronous and decentralized network, total bandwidth utilization by all network users, and potentially secure and uncongested data transmission make OCDMA very attractive for usage in all-optical local and metropolitan area networks. Multiuser interference (MUI) is a major obstacle in achieving high spectral efficiencies in OCDMA network transmission, and various approaches have been proposed in the literature to address this problem [1]–[11]. However, the vast majority of prior work in literature considers *chip-synchronous* bit-asynchronous OCDMA, since the assumption of *chip synchronism* gives rise to the worst-case MUI on the chip level.

This paper considers *chip-asynchronous* OCDMA transmission, when users transmit without any coordination; this entails that even the short chip intervals of arriving users are misaligned in time. In particular, we focus on the chip-asynchronous OCDMA channel with optical intensity modulation used at the transmitter and direct detection of optical signals at the receiver. We also assume *single-user demodulation* at the receiver due to receiver complexity constraints. Interestingly, it turns out that appropriate nonuniform signaling on the continuous-time binary *chip-asynchronous* OCDMA channel can lead to high spectral efficiencies of up to 2.5 bits per OCDMA chip.

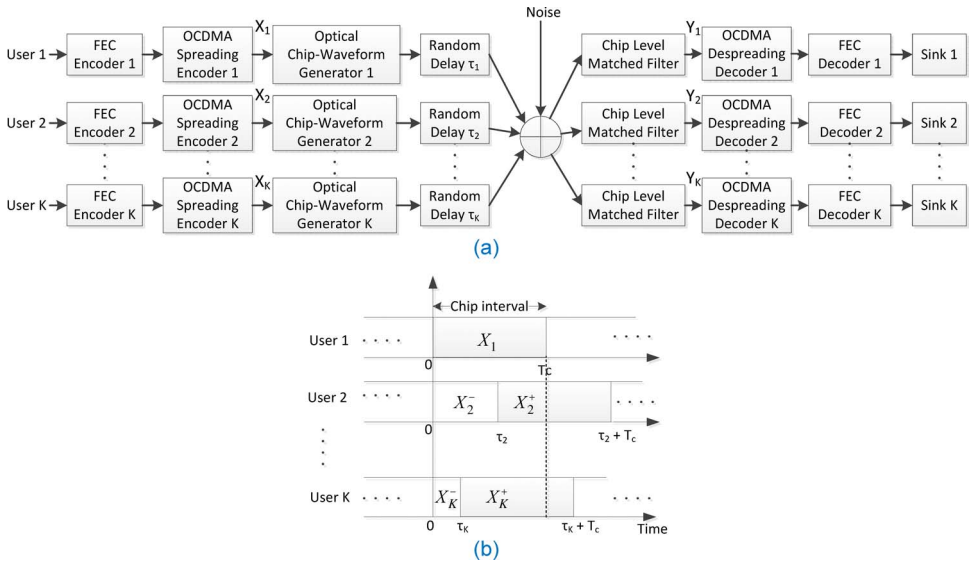

Fig. 1. Chip-asynchronous OCDMA transmission (a) Schematic block diagram showing considered network architecture (b) Previous and current symbols from interfering users affecting chip symbol X_1 of user 1.

The rest of this paper is organized as follows: The next section presents a construction of the chip-asynchronous binary OCDMA channel model used in our paper. Section 3 presents numerical capacity results illustrating the achieved capacity improvements of *chip-asynchronous* OCDMA when compared with *chip-synchronous* OCDMA. It also investigates the MUI on the channel and discusses results related to noise robustness of the optimal signaling scheme. Section 4 concludes this paper and presents directions of future work.

2. Channel Model for OCDMA With Random Chip Delays

Fig. 1(a) illustrates binary OCDMA transmission architecture with single-user demodulation at the receiver where K-independent and symmetric users transmit using OCDMA chip-symbols "0" and "1" (users do not collaborate and the probabilities of sending a "0" or a "1" are identical for all users). Each user's data bits are first error control coded and spread by an appropriate time-spreading OCDMA encoder, e.g., a time-hopping, a Pulse Position Modulation, or a Direct Sequence OCDMA spreading encoder. Resulting chip-symbols are then converted into continuous-time optical waveforms using intensity modulation by the optical-waveform generator. These waveforms are then transmitted over the optical-fiber link (e.g., using a star coupler) using On-Off Keying (OOK) modulation. Since all users transmit signals independently from different locations without any synchronization or cooperation, waveforms from different users are assumed to be received with different delays $\tau_1, \tau_2, \ldots, \tau_K \in [0, T_c]$, where T_c is the OCDMA chip-duration. In this paper, we assume τ_k are independent, uniformly distributed on $[0, T_c]$, and known to the receiver. During the modulation, transmission, and demodulation processes, the optical signals are assumed to add up incoherently without any beating. At the receiver, optical intensity direct detection is used assuming perfect photon counting processes.

For a K-user continuous-time channel with desired user 1 having delay $\tau_1 = 0$, the combination of all waveforms arriving at the receiver can be written as

$$y(t) = X_1 c(t) + \underbrace{\sum_{k=2}^{K} X_k^- c(t + T_c - \tau_k) + X_k^+ c(t - \tau_k)}_{\text{Total MUI signal affecting user 1}} + n(t), \qquad t \in [0, T_c] \tag{1}$$

where X_1 is the binary chip symbol sent by user 1, c(t) is the chip waveform used by all network users, X_k^- and X_k^+ are the previous and current symbols of the k^{th} interfering user, as shown in Fig. 1(b), and n(t) is the continuous-time noise corrupting the received signal. We make the standard OCDMA assumption that all users use the same chip waveform c(t), while differing in their used spreading encoders, the latter allowing a receiver to tune to a particular user. At the receiver shown in Fig. 1(a), the arriving continuous-time waveform y(t) then undergoes optical chip-level matched filtering, taking into account the delay of the desired user 1. If we consider the case of the chip waveform being a unit-intensity rectangular pulse on the chip interval $[0, T_c]$, then the resulting discrete-time channel output Y_1 for target user 1 is

$$\begin{aligned} Y_1 &= \frac{1}{T_c}\int_0^{T_c} y(t)\,dt \\ &= X_1 + \underbrace{\sum_{k=2}^{K}\left(\frac{\tau_k}{T_c}X_k^- + \left(1-\frac{\tau_k}{T_c}\right)X_k^+\right)}_{\text{total MUI seen by user 1}} + N_1 \end{aligned} \tag{2}$$

where N_1 is the discrete-time noise sample after matched filtering. The channel input chip symbol X_1 incorporates both the effect of spreading encoding and error control encoding performed by user 1. Furthermore, the same applies also for all interfering chip symbols $X_2^-, X_2^+, X_3^-, \ldots, X_K^+$ in the channel model from (2), i.e., these chip symbols incorporate the effects of different spreading encoders and error control encoding utilized by the interfering users 2, 3, ..., K, respectively, as shown in Fig. 1(a). (Note that, in the special case of OCDMA with pseudorandom spreading, chip symbol X_k would be a product of an error-control coded bit from user k and the spreading symbol c_k used by this user at a particular time instant.) Further channel output symbols for the first user are obtained by chip-level matched filtering during time intervals $[T_c, 2T_c], [2T_c, 3T_c], \ldots, [(n-1)T_c, nT_c]$, etc. Consequently, the output symbols from the chip-level matched filter are passed through a *chip-level* OCDMA spreading decoder of user 1, as shown in Fig. 1(a). (It should be highlighted that *chip-level* OCDMA spreading decoders presented in [3] and [8] would be applicable, while the traditional *bit-level* matched filter relying on Gaussian approximation of the MUI would not work.) Finally, the OCDMA spreading decoder is then followed by an error control decoder to recover the originally transmitted information bits of user 1.

3. Optimum Nonuniform Signaling for Binary Chip-Asynchronous OCDMA

The main objective of this section is to investigate the upper limit on the aggregate data throughput of the K-user binary chip-asynchronous OCDMA channel. The symmetric sum capacity is used as a metric for this upper limit. This section presents channel sum capacity results, insights into the near capacity MUI distribution, and the effect of additive noise in the OCDMA network.

The methodology used to obtain numerical results for the general case of random signal delays is based on an averaging principle. All numerical results are obtained by averaging one hundred sample results, each of which is obtained for an independent realization of random user delays $\tau_2, \tau_3, \ldots, \tau_K$. (Each τ_k is independently chosen from the uniform distribution $[0, T_c]$.) When generating results for independent realizations of random delays, the limitations of time resolution in practical systems are taken into account by quantizing the chip duration T_c to N time subintervals. Individual user delays τ_k then take values $n * (T_c/N)$, where n is an integer taking values from a uniform distribution between 1 and $N-1$. Throughout this paper, numerical results are generated with a choice of $N = 1000$.

3.1. Binary Channel Capacity

Using the chip-asynchronous channel model from (2) in the previous section, the maximum rate of reliable information transfer on the binary *chip-asynchronous* OCDMA channel was determined.

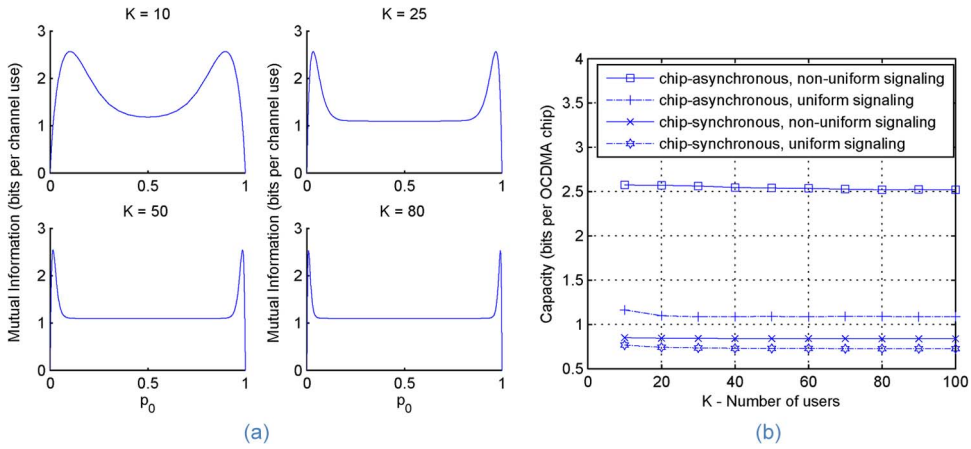

Fig. 2. (a) Mutual information as a function of the probability of sending a "0" chip symbol for *chip-asynchronous* OCDMA. (b) OCDMA sum capacity as a function of number of users K for chip-asynchronous transmission compared with chip-synchronous transmission.

TABLE 1

Sum capacity values and corresponding capacity achieving probabilities from plots in Fig. 2(a)

K	Capacity (bits per OCDMA chip)	Capacity Achieving Probabilities
10	2.5671	p_0=0.900 and p_1=0.100
25	2.5657	p_0=0.968 and p_1=0.032
50	2.5432	p_0=0.986 and p_1=0.014
80	2.5246	p_0=0.991 and p_1=0.009

Numerical evaluation of the symmetric *sum capacity* was carried out by maximizing appropriate mutual information over all possible channel input probability mass functions

$$C = K \times \sup_{P_{X_1}} I(X_1; Y) \text{ bits per channel use.} \tag{3}$$

Fig. 2(a) shows the above mutual information $K \times I(X_1; Y)$ as a function of probability of sending the "0" symbol for $K = 10$, 25, 50, and 80 channel users. The effects of any additive noise have been neglected in this subsection. It can be observed that, while the mutual information is nearly constant in the middle portions of the plots, Fig. 2(a) shows a significant rise on the sides of the plots. Consequently, the optimum signaling probabilities are nonuniform. Table 1 summarizes the values of capacity peaks and corresponding capacity achieving probabilities from Fig. 2(a) for $K = 10$, 25, 50, and 80 users. One can observe that, for large values of K, the following nonuniform probabilities achieve near-capacity transmission in the considered *chip-asynchronous* case:

$$p_0 \approx \frac{K - 0.7}{K}, \; p_1 \approx \frac{0.7}{K}. \tag{4}$$

However, it is interesting to see that, in the *chip-synchronous* case, the following nonuniform probability distribution achieves near-capacity transmission:

$$p_0 \approx \frac{K - 1.2}{K}, \; p_1 \approx \frac{1.2}{K}. \tag{5}$$

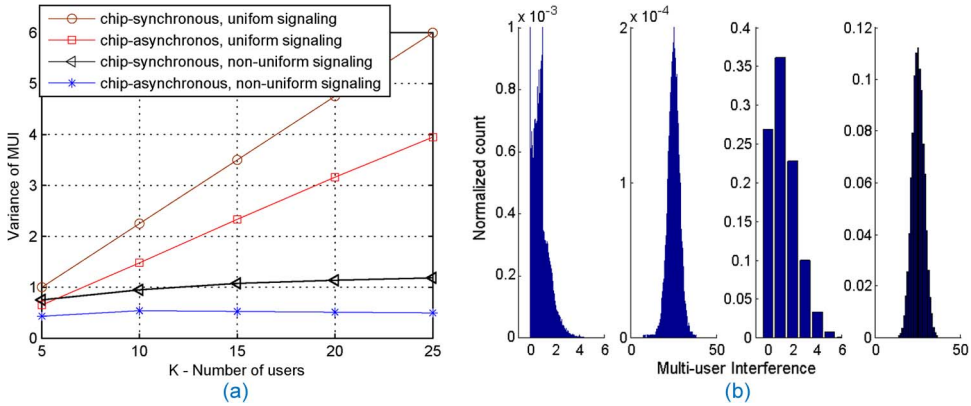

Fig. 3. MUI in chip-asynchronous binary OCDMA with nonuniform signaling. (a) Variance of MUI vs. the number of OCDMA network users, K. (b) Normalized histograms of channel MUI with $K = 50$ users for different cases (left to right): Near capacity nonuniform signaling in the chip-asynchronous case; Uniform signaling in the chip-asynchronous case; Near capacity nonuniform signaling in the chip-synchronous case; Uniform signaling in the chip-synchronous case.

Fig. 2(b) presents the sum capacity of OCDMA transmission against the number of users K for various transmission scenarios. One can observe that an asymptotic capacity of about 2.5 bits per chip is achieved by nonuniform signaling on the *chip-asynchronous* OCDMA channel. Furthermore, it can be deduced that the reason for achieving this high OCDMA capacity is shared by both the chip asynchronism and the appropriate nonuniform signaling. In particular, uniform signaling on the same *chip-asynchronous* channel yields only an asymptotic capacity of about 1.07 bits per channel use. On the other hand, for nonuniform signaling on the *chip-synchronous* channel, the asymptotic capacity reaches about 0.84 bits per channel use. Finally, Fig. 2(b) also shows that the widely considered uniform signaling for *chip-synchronous* OCDMA achieves a capacity of 0.72 bits per OCDMA chip.

One can observe in Fig. 3(b) that, in the *chip-asynchronous* case, the capacity achieving MUI has a mixed non-Gaussian distribution, while in the *chip-synchronous* case, the capacity-achieving MUI is asymptotically Poisson distributed. Subsequently, the capacity of chip-asynchronous or chip-synchronous OCDMA is not achieved by minimizing the amount of channel MUI, as might be intuitively reasoned. Had this been the case, the capacity achieving p_1 would be 0, as it causes the least amount (none) of MUI. However, for $p_1 = 0$, the mutual information on the channel is clearly 0 in Fig. 2(a), so such p_1 is not capacity achieving.

3.2. Variance and Distribution of the MUI on the OCDMA Channel

To gain insight into the results of higher capacity achieved in the binary *chip-asynchronous* OCDMA network through nonuniform signaling, the variance of the MUI can be derived using the channel model from (2)

$$\mathrm{var}(\mathrm{MUI})_{\mathrm{chip-asynch.}} = \mathrm{var}\left(\sum_{k=2}^{K}\left(\frac{\tau_k}{T_c}X_k^- + \left(1-\frac{\tau_k}{T_c}\right)X_k^+\right)\right) \tag{6}$$

$$= \sum_{k=2}^{K}\mathrm{var}\left(\frac{\tau_k}{T_c}X_k^- + \left(1-\frac{\tau_k}{T_c}\right)X_k^+\right) \tag{7}$$

$$= \sum_{k=2}^{K}\mathrm{E}\left(\left(\frac{\tau_k}{T_c}X_k^- + \left(1-\frac{\tau_k}{T_c}\right)X_k^+\right)^2\right) - \left(\mathrm{E}\left(\frac{\tau_k}{T_c}X_k^- + \left(1-\frac{\tau_k}{T_c}\right)X_k^+\right)\right)^2 \tag{8}$$

$$= \frac{2}{3}(K-1)(p_1 - p_1^2) \tag{9}$$

where (7) follows due to independence of the users and (9) follows from user delays τ_k being uniformly distributed. For comparison, we also evaluate the variance in the chip-synchronous case $(\tau_1 = \tau_2 = \ldots = \tau_k = 0)$ as

$$\text{var}(\text{MUI})_{\text{chip}-\text{synch.}} = \text{var}\left(\sum_{k=2}^{K} X_k^+\right) \tag{10}$$

$$= \sum_{k=2}^{K} \text{var}\left(X_k^+\right) \tag{11}$$

$$= \sum_{k=2}^{K} \text{E}\left(\left(X_k^+\right)^2\right) - \left(\text{E}\left(X_k^+\right)\right)^2 \tag{12}$$

$$= (K-1)\left(p_1 - p_1^2\right) \tag{13}$$

where (11) follows due to independence of interfering users and (13) follows from X_k^+ being Bernoulli distributed. In the *uniform signaling* case, i.e., $p_0 = p_1 = 0.5$, the above expressions can be evaluated to

$$\text{var}(\text{MUI})_{\text{chip}-\text{asynch.}}^{\text{uniform}} = \frac{K-1}{6} \tag{14}$$

$$\text{var}(\text{MUI})_{\text{chip}-\text{synch.}}^{\text{uniform}} = \frac{K-1}{4}. \tag{15}$$

Finally, it is interesting to observe that, for *nonuniform signaling* and a large number of users K

$$\text{var}(\text{MUI})_{\text{chip}-\text{asynch.}}^{\text{nonuniform}} = \left(\frac{2}{3}(K-1)\left(\frac{0.7}{K} - \left(\frac{0.7}{K}\right)^2\right)\right) \longrightarrow \frac{7}{15} \approx 0.47 \tag{16}$$

$$\text{var}(\text{MUI})_{\text{chip}-\text{synch.}}^{\text{nonuniform}} = \left((K-1)\left(\frac{1.2}{K} - \left(\frac{1.2}{K}\right)^2\right)\right) \longrightarrow \frac{6}{5} = 1.20 \tag{17}$$

for the capacity optimal channel input probabilities from (4) and (5).

Fig. 3(a) plots the numerically evaluated MUI variance against the number of OCDMA users K for both, the *chip-synchronous* and *chip-asynchronous* cases. Note that there is a perfect match between the numerically evaluated results and the analytically derived MUI variance expressions. Equations (9) and (13) evaluated using exact capacity achieving probabilities match the variance values in Fig. 3(a) for the nonuniform signaling case, whereas for uniform signaling, (14) and (15) match the uniform signaling plots of Fig. 3(a). The lowest MUI variance is achieved by using appropriate nonuniform signaling on the *chip-asynchronous* channel, supporting the highest channel capacity value in Fig. 2(b). Larger values of MUI variance are observed with nonuniform signaling on the *chip-synchronous* channel. However, contrary to the nonuniform signaling cases, MUI variance in case of uniform signaling increases with the number of users for both the chip-synchronous and chip-asynchronous transmission scenarios. Overall, MUI variance levels observed in Fig. 3(a) strongly support the different capacity curves in Fig. 2(b).

Fig. 3(b) aims to reveal further insight into the interference on the channel by comparing distributions of the normalized MUI in different cases that this paper considers. This figure illustrates that the MUI distribution is strictly non-Gaussian when the optimized nonuniform signaling is used in the *chip-asynchronous* case. Moreover, it also shows that the variance of the channel MUI in this case is lower compared with the variance of capacity achieving non-Gaussian MUI distribution obtained with nonuniform signaling in the *chip-synchronous* case. The near-Gaussian shape taken by MUI distributions resulting from uniform signaling in the *chip-asynchronous* and *chip-synchronous* cases are also shown in Fig. 3(b). The fact that Gaussian interference is the worst supports the higher capacity achieved by nonuniform signaling in the chip-asynchronous case (where interference is non-Gaussian).

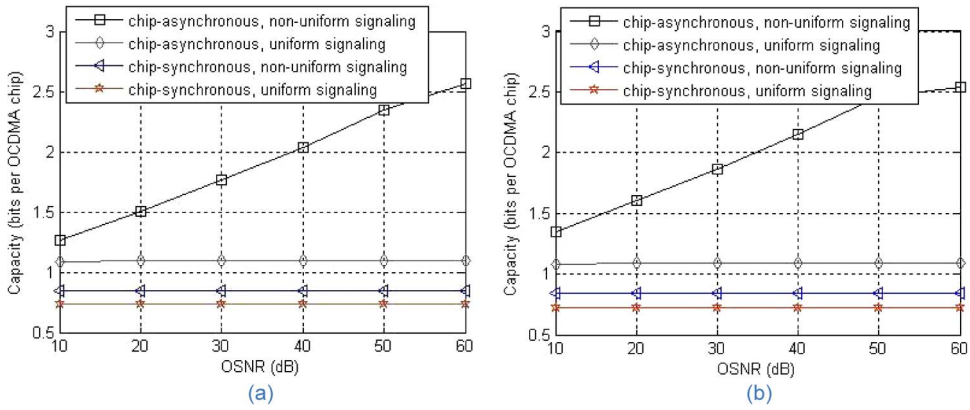

Fig. 4. Capacity vs. OSNR curves for (a) K = 30 users (b) K = 70 users on the channel.

3.3. Robustness of Capacity Gains to Additive Noise

In a practical system, the single-user receiver will be affected by external noise in addition to the MUI on the channel. In this subsection, we consider the case where thermal noise from receiver electronics is the dominant external noise. Then, in (2), N_1 would be a Gaussian random variable with mean 0 and variance σ^2. Consequently, the conditional probability density function describing the OCDMA channel is given by

$$f_{(Y_1|X_1)}(y_1|x_1) = \sum_{x_2^- x_2^+ x_3^- x_3^+ \ldots x_K^- x_K^+ \in \{0;1\}^{2K-2}} \left[\frac{1}{\sqrt{2\pi}\sigma} \exp\left(\frac{1}{2}\sigma^{-2} \left(y_1 - \left(\sum_{k=2}^{K} \frac{\tau_k}{T_c} x_k^- + \sum_{k=2}^{K} \left(1 - \frac{\tau_k}{T_c}\right) x_k^+ \right) \right)^2 \right) \times \prod_{k=2}^{K} P(X_k^- = x_k^-) P(X_k^+ = x_k^+) \right] \quad (18)$$

and the channel output density is given for all output values y_1

$$f_{Y_1}(y_1) = P(X_1 = 0) f_{Y_1|X_1}(y_1|x_1 = 0) + P(X_1 = 1) f_{Y_1|X_1}(y_1|x_1 = 1). \quad (19)$$

Numerical capacity evaluation was done using the probability density functions from (18) and (19) and obtaining *differential entropy* values through numerical integration. For intensity-based optical modulation, we define the chip-level optical signal-to-noise ratio as $\text{OSNR}_{\text{chip}} = \text{Symbol energy}/\text{Noise energy} = E(X_1)/\sigma^2$ and observe the change in throughput limit of OCDMA with increasing OSNR.

Fig. 4 shows channel capacity as a function of chip-level OSNR for $K = 30$ and 70 channel users, respectively. When compared with the noiseless case, a drop in capacity values is observed in the case of nonuniform signaling in the chip-asynchronous case. Nevertheless, for practical optical SNRs between 30 and 40 dB, the capacity values are largely retained, e.g., at 35-dB SNR, the capacity with 30 users is 1.9, whereas in the 70-user case, it is 2 bits per OCDMA chip. Compared with the result of 0.82 bits per OCDMA chip in the noiseless chip-synchronous case with nonuniform signaling, this is higher than a 2.3 times gain. Thus, the capacity increase due to nonuniform signaling in the chip-asynchronous case is robust to thermal noise levels observed in practical scenarios.

4. Conclusion

This paper has presented results for *chip-asynchronous* binary OCDMA channel with users being affected by uniformly distributed random chip delays relative to each other. It has been shown that,

through optimized nonuniform signaling on such a *chip-asynchronous* channel, high spectral efficiencies of up to 2.5 bits per chip are achievable. This is a threefold increase in OCDMA capacity when compared with the best reported *chip-synchronous* binary OCDMA capacity.

It has been also highlighted that the use of capacity-achieving nonuniform signaling leads to a non-Gaussian MUI with significantly lowered variance. The capacity gains have been shown to be robust to reasonable levels of additive noise. In summary, this paper has established that significantly higher transmission rates can be achieved in OCDMA networks by properly accounting for inherent *chip-asynchronism* therein. Our future work is focused toward the study of achievable capacities if M-ary symbols are transmitted on the chip-asynchronous OCDMA channel and design of coded OCDMA systems with near capacity performance.

References

[1] P. R. Prucnal, *Optical Code Division Multiple Access: Fundamentals and Applications*. Boca Raton, FL, USA: CRC Press, 2006.

[2] T. Ohtsuki, "Performance analysis of direct-detection optical asynchronous CDMA systems with double optical hard-limiters," *J. Lightw. Technol.*, vol. 15, no. 3, pp. 452–457, Mar. 1997.

[3] H. M. H. Shalaby, "Chip-level detection in optical code division multiple access," *J. Lightw. Technol.*, vol. 16, no. 6, pp. 1077–1087, Jun. 1998.

[4] E. Inaty, L. A. Rusch, and P. Fortier, "Multirate optical fast frequency hopping CDMA system using power control," in *Proc. IEEE Global Telecommun. Conf.*, Nov. 2000, pp. 1221–1227.

[5] H. M. H. Shalaby, "Complexities, error probabilities, and capacities of optical OOK-CDMA communication systems," *IEEE Trans. Commun.*, vol. 50, no. 12, pp. 2009–2017, Dec. 2002.

[6] A. J. Mendez, R. M. Gagliardi, V. J. Hernandez, C. V. Bennett, and W. J. Lennon, "Design and performance analysis of wavelength/time (W/T) matrix codes for optical CDMA," *J. Lightw. Technol.*, vol. 21, no. 11, pp. 2524–2533, Nov. 2003.

[7] T. B. Osadola, S. K. Idris, I. Glesk, and W. C. Kwong, "Network scaling using OCDMA over OTDM," *IEEE Photon. Technol. Lett.*, vol. 24, no. 5, pp. 395–397, Mar. 2012.

[8] A. A. Garba and J. Bajcsy, "Using turbo codes and non-Gaussian interference to improve spectral efficiency in M-ary optical CDMA networks," in *Proc. Int. Symp. Turbo Codes Relat. Topics*, Apr. 2006, pp. 1–6.

[9] A. A. Garba and J. Bajcsy, "A new approach to achieve high spectral efficiency in wavelength-time OCDMA network transmission," *IEEE Photon. Technol. Lett.*, vol. 19, no. 3, pp. 131–133, Feb. 2007.

[10] A. A. Garba, J. Bajcsy, and S. A. Khan, "An asymptotic lower bound on the capacity of M-ary CDMA transmission with non-Gaussian multi-user interference," in *Proc. of IEEE Int. Conf. Telecommun.*, Apr. 2010, pp. 29–35.

[11] A. A. Garba and J. Bajcsy, "Optical code division multiple access network transmission with M-ary chip symbols," *IEEE/OSA J. Opt. Commun. Netw.*, vol. 3, no. 5, pp. 435–446, May 2011.

[12] A. A. Farid and S. Hranilovic, "Channel capacity and non-uniform signaling for free-space optical intensity channels," *IEEE J. Sel. Areas Commun.*, vol. 27, no. 9, pp. 1553–1563, Dec. 2009.